

KMS Technologies – KJT Enterprises Inc.

He, Z., Wang, Z., Yu, G., Strack, K.M., and Liu, H.

Modeling of 3D MCSEM and sensitivity analysis

2007

Publication copy

PIERS online, 3 (5)

Modeling of 3D MCSEM and Sensitivity Analysis

Zhanxiang He^{1,2}, Zhigang Wang², Gang Yu³, Kurt Strack³, and Haiying Liu²

¹Department of Geosciences, University of Houston, USA

²BGP CNPC, China

³KMS Technologies — KJT Enterprises, Inc, USA

Abstract— After decades of research and development, Marine Controlled Source Electromagnetic (MCSEM) has come into the application phase. It has shown good practical effect, but the 3D modeling is far from practical stage. Based on the modeling of 3D frequency-domain MCSEM to a complicated target body and sensitivity analysis, a method which can quantitatively delimit boundary of anomaly body is described in the paper. For air-wave-dominated far field zone, we suggest to adopt the theory of plane wave to calculate apparent resistivity thereby improving the adaptability of the method.

DOI: 10.2529/PIERS060905213154

1. INTRODUCTION

In the past decades of years, the theoretical research and practical application of MCSEM have undergone hard process. The initial research began early in 1970's [1], but only in the recent years when digital instrument [3, 6], data processing algorithm [7] and interpretation method are significantly developed, MCSEM came into application phase [2–5, 8]. Presently, the widely adopted inversion is 1D. Although 1D inversion result is approximate, it is very useful [9]. In 2004, Mittet and Ellingsrud (2004) released their 1D inversion algorithm and result, which indicates that 1D inversion can identify hydrocarbon layer.

In 2002, Eidesmo used 2D finite element algorithm to study boundary effect of MCSEM (Eidesmo, et al., 2001). Because the 2D EM modeling is not a suitable method to describe anomaly feature, it is seldom used in MCSEM, and the general used is 3D modeling. In recent years, 3D modeling of MCSEM has been developed rapidly. Numerous 3D modeling algorithms are brought forward, therewith Zhdanov from Utah University is a representative. Ueda adopted quasi-linear approximate algorithm to do rapid CSEM modeling [11] thereby remarkably speeding calculation and ensuring precision. The algorithm gives good result to practical data. When there is more than one source, it consumes more time. Zhdanov and Wan (2005) use 3D integral equation algorithm to do CSEM modeling to complex model with inhomogeneous background. As a result, the hydrocarbon reservoir is accurately imaged with constrain from known salt dome or volcanic body. Zhdanov and Wan (2005) also used the algorithm to do rapid migration image to MCSEM data. The result indicates that the algorithm is an effective method for imaging submarine resistive body. In addition, Zhdanov and Yoshioka (2005) have done 3D iteration inversion to MCSEM data.

Modeling of time-domain MCSEM is late than that of frequency-domain, but according to 1D and 3D modeling results released by Um and Alumbaugh (2005), the time-domain EM is sensitive to small-sized reservoir. When pulse period and T-R spacing are selected suitably, noise can be significantly suppressed and data precision can be improved. It can also reduce the influence of air wave to time-domain EM field in shallow water.

The paper presents the remarkable improvement on the practicability of the algorithm based on the 3D integral equation algorithm presented by Zhdanov. The improved algorithm can realize the modeling of complex practical data. In addition, an approximate quantitative method delimiting resistive body is presented in the paper based on the modeling to different models. The paper also discussed how to make frequency-domain CSEM method effective in the air-wave-controlled environment.

2. CREATING OF COMPLEX MODEL FOR INTEGRAL EQUATION ALGORITHM

Zhdanov recently presented an integral equation algorithm which can realize the modeling to a model with inhomogeneous background. The algorithm adopts Green function to calculate the response of an 1D horizontal layered model. It can also conduct 3D EM modeling to the model

with inhomogeneous resistivity background. The modeling result to a geology model composing several anomaly bodies which have the same geo-electric feature also is presented in the paper. The algorithm shows considerable application foreground. But in the paper there is no detailed description about how to create practically complex model.

The program to rapidly create a 3D resistivity model from reservoir model or from practical 3D seismic-data is presented in the paper. At first, 1D background model and inhomogeneous resistivity background model are constructed individually based on known data. Secondly, construct a target model or practical model based on 3D seismic data and logging data on reservoir zone. Regional or known geology body is usually taken as inhomogeneous resistivity background thereby minimizing target model. For example, for the model composing only one reservoir zone, not only all meshes within reservoir but also those out of reservoir may be evaluated by variable resistivity according to the actual condition. If the model composes several reservoir zones, meshes within different reservoir zone may be evaluated individually.

3. HOW TO MAP THE BOUNDARY OF RESISTIVE RESERVOIR

For frequency-domain CSEM, the most significant figure to study resistive reservoir is MVO (Magnitude Versus Offset) curve which can display the variation of anomaly magnitude or phase as a function of offset. Whatever the geo-electric structure is, magnitude of electrical field will attenuate when source and receiver offset (Tx-Rx spacing) increases. But hydrocarbon model will exhibit significant different character from non-hydrocarbon model on MVO curve. Figure 1 displays two different MVO curves. The boundary of reservoir is at 5 km. The black curve corresponds to hydrocarbon model while the red one to the non-hydrocarbon model. The two curves exhibit significant difference. The generalization curve (Figure 2) shows apparent high magnitude indicating the resistive reservoir. Either MVO curve or generalized curve can only indicate the existence of hydrocarbon reservoir and can not map the reservoir boundary, but on the MVO

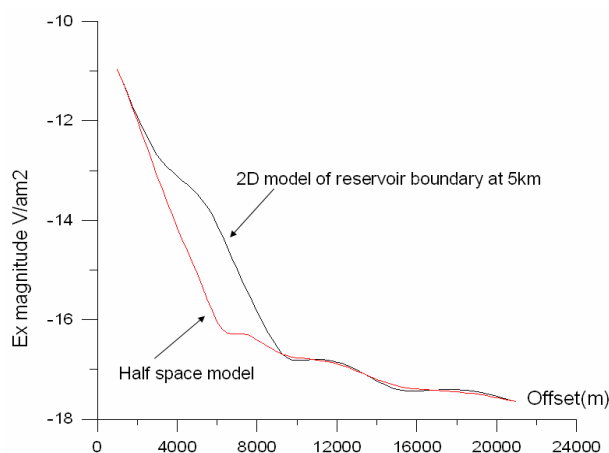


Figure 1: MVO curves.

second derivative curve (MVOSD) (Figure 3) it can be found that reservoir boundary exhibit apparent and approximately stable character, i.e., the first zero point is located within the resistive body while the second extremum appears about 0.5 km away from hydrocarbon boundary. To get the common rule, we modeled numerous models. Figure 4 displays a model composing a $50 \times 50 \text{ km}^2$ square reservoir. The source is positioned at the center of one boundary. When source-receiver offset crosses the boundary, the MVO curves (Figure 5) for models with different lateral extension (from 3 km to 11 km) show different characters. When the offset is small, the dominated field is the reflected wave. At this small offset, the MVO curves for half-space model, 2D model and 3D model overlay each other. With the increasing of offset, the reflected field from underlying layer gradually begins to influence the MVO curve thereby making the curve going upwards. The wider the side length of the reservoir, the higher the curve goes upwards. But with the continual increasing of the offset, the influence from air wave increases accordingly. When air wave takes the dominative position, MVO curves overlay again. On the figure, it is indicated that the curves for models with different lateral extensions and 1D model joint at a point which corresponds to the boundary of resistive reservoir. Figure 6 is the MVOSD curve. The MVOSD curves for reservoirs with different scale show approximately similar character while neither half-space model nor 2D model exhibits this kind of character. Especially, the second extreme point always appears about 0.5 km away from the boundary of resistive reservoir. The third extreme point indicates another boundary of reservoir. Based on these characters, reservoir boundary can be delimited. Much modeling calculation indicates that the second extreme point of MVOSD curve will not move when source frequency, target depth and thickness, seabed depth, even the resistivity of target vary if the resistive reservoir is detectable. Therefore, the extremeum is an indicator of the boundary of resistive reservoir.

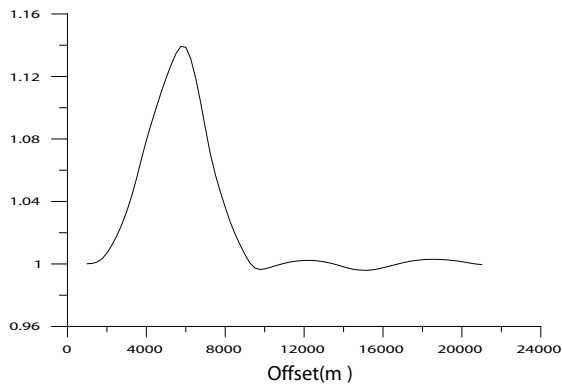


Figure 2: Generalized MVO curve.

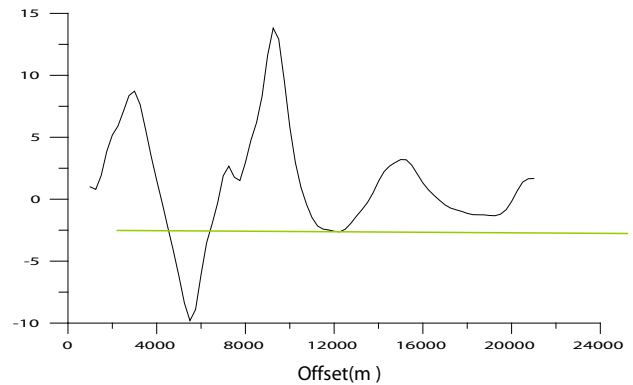


Figure 3: MVOSD curve for boundary at 5 km model.

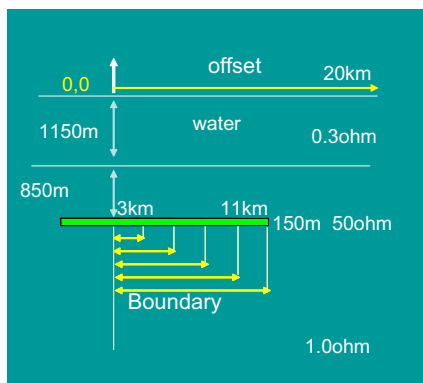


Figure 4: Sketch for models with different size.

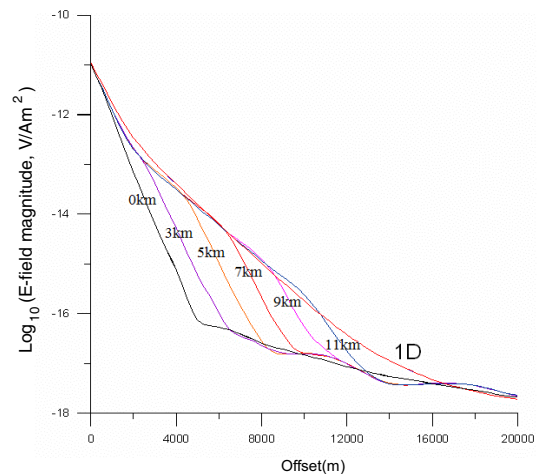


Figure 5: MVO curves for models with different size.

4. MAPPING THE BOUNDARY OF SEVERAL RESERVOIR LAYERS ALONG VERTICAL DIRECTION

How to recognize anomaly bodies by MVO and MVOSD curves when there is more than one resistive body at different depths? Under the situation, MVO curve is powerless. It can only indicate the existence of resistive bodies but can't recognize these anomaly bodies individually. As for MVOSD curve, it can not recognize the lower anomaly bodies if the upper resistive body is larger than the lower one(s). But if the upper body is smaller than the lower one and the boundary of the lower body is located out of the boundary of the upper body, the second derivative curve will appear two apparent extreme points which correspond to the boundaries of the two resistive bodies respectively. If the two resistive bodies are located near, the two extreme points will joint at one point which indicates the boundary of the larger anomaly body. Figure 7 displays the MVOSD curves for three models. It clearly displays the phenomenon. (Explain Figure 7 here).

5. HOW TO DELIMIT RESISTIVE BODY WHEN T-R SET IS POSITIONED FAR FROM IT

If T-R set does not cross resistive body or the source is positioned far away from the resistive body and source-receiver spacing is large, the signal will be dominated by air wave after a long transmission. Therefore, MVO or MVOSD curve does not exhibit any anomaly. How to recognize the resistive body under this situation? Someone may think that the frequency-domain CSEM is powerless at this situation. But our modeling results still can recognize the resistive body under this situation. Because the excited field is mainly plane wave, Cagniard resistivity can be calculated just like ground CSAMT, and the resistive body can be delimited based on apparent resistivity profile. If we continue to do inversion on the profile, spatial distribution of the resistive body can be mapped. Figure 8 shows the apparent resistivity profile. On the profile a high resistivity zone appears at the center. The generalization profile (Figure 8(b)) indicates boundary of the resistive body in more detail.

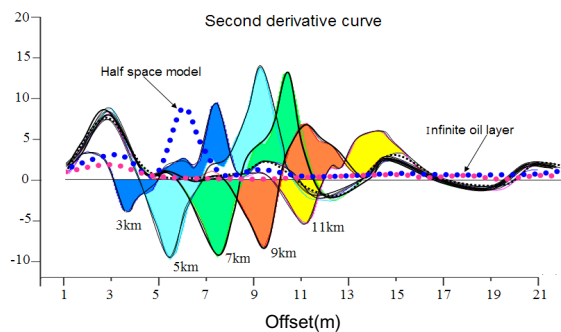


Figure 6: Second derivative curve of MVO for models with different size.

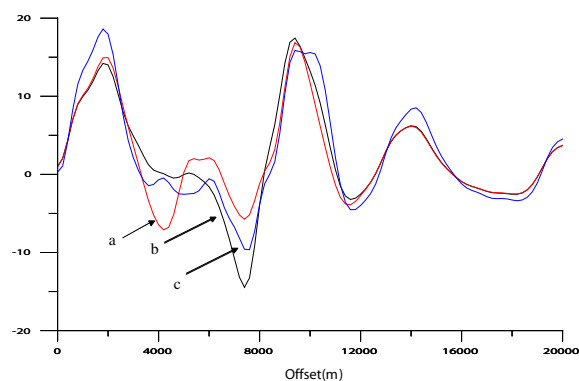


Figure 7: MVOSD curves for a model composing three resistive bodies Vertically. a. The upper resistive body is 4 km wide, the lower 7 km wide, b. The upper resistive body is 7 km wide, the lower 4 km wide, c. The upper resistive body is 3 km wide, the middle 5 km wide.

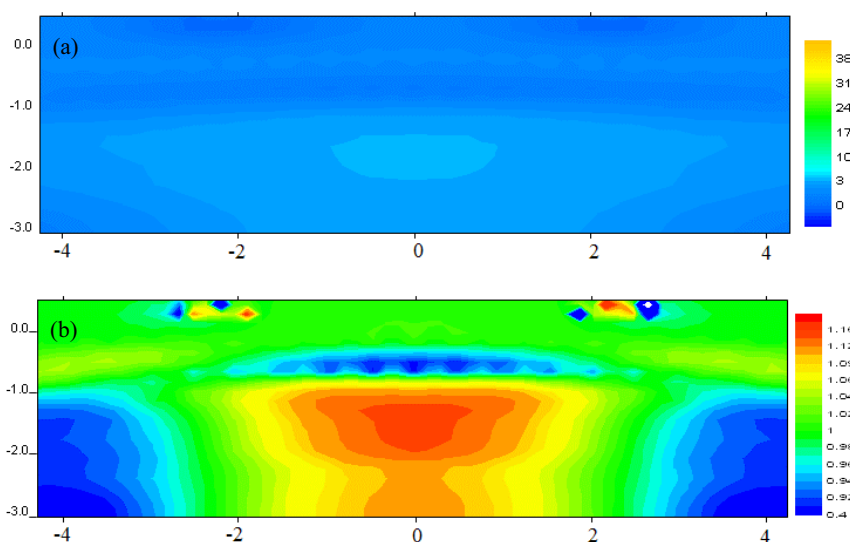


Figure 8: (a) Apparent resistivity profile (b) Generalized resistivity profile.

6. CONCLUSION

Frequency-domain MCSEM is one of the major EM methods applied on marine oil and gas exploration. It has been proved successfully by many oil companies and service companies. But the data processing still stays in qualitative stage. Theoretically, MVOSD curve can accurately delimit reservoir, but practically the precision is limited by the precision of observed data. Therefore, if observed data have high quality and precision, it is an effective means to delimit resistive body. When MVO curve is powerless due to air wave, theory of plane wave can help to calculate apparent resistivity. At all events, rapid 3D inversion is an important step of data processing and interpretation for successful MCSEM survey.

ACKNOWLEDGMENT

We greatly appreciate Dr. Shenghui Li for his helpful advice and technical discussion and Prof. Hua-Wei Zhou as advisor & his help.

REFERENCES

1. Cox, C. S., J. H. Filloux, and J. Larsen, "Electromagnetic studies of ocean currents and electrical conductivity below the ocean floor," *The Sea*, Vol. 4, Part I, 637–693, ed. Maxwell (ed.), Wiley, 1971.
2. Constable, S. and C. S. Cox, "Marine controlled source electromagnetic sounding 2, The PEGASUS experiment," *Journal of Geophysical Research*, Vol. 101, 5519–5530, 1996.

3. Constable, S., A. Orange., G. M. Hoversten, and H. F. Morrison, "Marine magnetotellurics for petroleum exploration 1. A seafloor instrument system," *Geophysics*, Vol. 63, 816–825, 1998.
4. Hoversten, G. H., H. F. Morrison, and S. Constable, "Marine magnetotellurics for petroleum exploration 2. Numerical analysis of subsalt resolution," *Geophysics*, Vol. 63, 826–840, 1998.
5. Hoversten, G. H., S. Constable, and H. F. Morrison, "Marine magnetotellurics for base salt mapping: Gulf of Mexico field-test at the Gemini structure," *Geophysics*, Vol. 65, 1476–1488, 1999.
6. Heinson, G., S. Constable, and A. White, "Episodic melt transport at a mid-ocean ridge inferred from magnetotelluric sounding," *Geophys. Res. Lett.*, Vol. 18, 1917–1920, 2000.
7. Tompkins, M. J., A. Greer, N. Barker., R. Weaver, and L. M. MacGregor, "Effects of vertical anisotropy on marine active source electromagnetic data and inversions," *66th EAGE Annual Meeting*, Paris, France, 7–10 June, 2004.
8. MacGregor, L., M. Sinha, and S. Constable, "Electrical resistivity structure of the Valu Fa Ridge, Lau Basin, from marine controlled-source electromagnetic sounding," *Geophys. J. Int.*, Vol. 146, 2001.
9. Eidesmo, T., S. Ellingsrud, etc., "Sea Bed Logging (SBL), a new methods for remote and direct identification of hydrocarbon filled layers in deepwater areas," *First Break*, Vol. 20, 144–152, 2002.
10. Mittet, R., L. Løseth, and S. Ellingsrud, "Inversion of SBL data acquired in shallow waters Paris," *66th EAGE Conference & Exhibition*, France, June 2004.
11. Ueda, T. and M. S. Zhdanov, "Fast numerical modeling of marine controlled-source electromagnetic data using quasi-liner," *75th SEG*, Houston, 2005.
12. Zhdanov, M. S. and S. K. Lee, "Integral equation method for 3D modeling of EM field in complex structures with inhomogeneous background conductivity in marine CSEM applications," *75th SEG*, Houston, 2005.
13. Zhdanov, M. S. and L. Wan, "Rapid seabed imaging by frequency domain EM migrateon," *75th SEG*, Houston, 2005.
14. Zhdanov, M. S. and K. Yoshioka, "3D iterative inverseon of the marine CSEM data," *75th SEG*, Houston, 2005.
15. Um, E. and D. Alumbaugh, "On the physics of the marine-time-domain controlled source electromagnetic method for detecting hydrocarbon reservoirs," *75th SEG Annual Conference*, 6–11 November, Houston, TX, 2005.

KMS Technologies – KJT Enterprises Inc.
6420 Richmond Ave., Suite 610
Houston, Texas, 77057, USA Tel:
713.532.8144

Please visit us
www.kmstechnologies.com